

# Principles for Measurement of Chemical Exposure Based on Recognition-Driven Anchoring Transitions in Liquid Crystals

Rahul R. Shah\* and Nicholas L. Abbott†

The competitive binding of a molecule forming a liquid crystal and a targeted analyte to a common molecular receptor presented at a solid surface possessing nanometer-scale topography is used to trigger an easily visualized surface-driven change in the orientation of a micrometer-thick film of liquid crystal. Diffusion of the targeted analyte from atmosphere to surface-immobilized receptor across the micrometer-thick film of liquid crystal is fast (on the order of seconds), and the competitive interaction of the targeted analyte and liquid crystal with the receptor provides a high level of tolerance to nontargeted species (water, ethanol, acetone, and hexanes). Systems that provide parts-per-billion (by volume) sensitivity to either organoamine or organophosphorus compounds are demonstrated, and their use for imaging of spatial gradients in concentration is reported. This approach does not require complex instrumentation and could provide the basis of wearable personalized sensors for measurement of real-time and cumulative exposure to environmental agents.

To understand accumulation and toxicity from environmental exposure, it is necessary to be able to selectively detect a variety of synthetic organic chemicals (1). Whereas highly sensitive methods of detection of specific chemical compounds do exist (2), these methods require laboratory-based instrumentation and thus are not suited for measurement of personal exposure (3). We report an alternative approach where surface-driven, orientational transitions in supported films of liquid crystals (LCs) (4–6) are triggered by exposure to parts-per-billion (ppb) vapor concentrations of targeted low molecular weight molecules, including organoamine and organophosphorus compounds. The recognition-driven change is used to visually detect instantaneous or cumulative exposure to a targeted compound. Fabrication of the detection system is sufficiently simple that it may find use as the basis of wearable personal sensors for exposure to environmental pollutants (7).

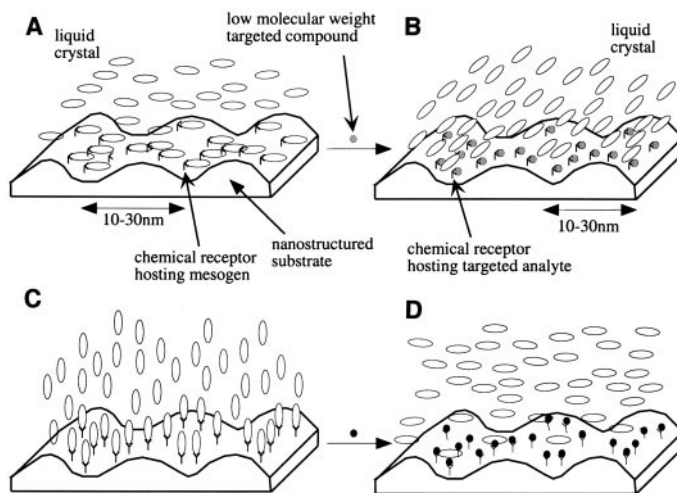
Three principles underlie the design of the detection system (Fig. 1) (8–10). First, the solid surface presents immobilized chemical receptors that weakly bind molecules that form a LC phase to orient it in a well-defined direction. Second, the receptors bind targeted analytes more strongly than they bind the molecules forming the LC. Here we exploit

knowledge of the relative strengths of hydrogen bond (11), acid-base (12), and metal-ligand coordination (13) interactions to guide selection of appropriate molecular receptors and LCs for each targeted analyte. The competitive displacement of the molecules forming the LC from the molecular receptor reversibly releases the LC from its receptor-enforced orientation upon exposure to analyte. Because nontargeted species that bind the receptors more weakly than the molecules that form the LC will not change the orientation of the LC, this competitive interaction provides a level of specificity for the targeted

analyte that is substantially greater than schemes based on noncompetitive binding of analytes to receptors (4–6, 14, 15). Third, the surface possesses a nanometer-scale topography that directs the LC to assume a predictable and visually distinct orientation in the absence of a receptor-mediated-anchoring of the mesogen at the surface (16).

For detection of organoamines (17), we use carboxylic acid (-COOH) groups as the molecular receptors and 4-cyano-4'-pentylbiphenyl (5CB) as the LC. Whereas the nitrile group of 5CB can hydrogen bond with a -COOH group [bond strength 10 to 40 kJ/mol (11)], an organoamine will bind with -COOH through a stronger acid-base interaction (>70 kJ/mol (12)). We prepared ultrathin gold films with a nanometer-scale topography and with protruding surface-immobilized -COOH groups (18). The topography of the surface can be idealized as a nanometer-scale corrugation with an amplitude of ~1 to 2 nm and a wavelength of 10 to 30 nm (19). When placed on this surface, 5CB will spontaneously assume an orientation that is parallel to the surface and perpendicular to (across) the nanometer-scale corrugation, consistent with the influence of hydrogen bonding of the nitrile group of the mesogen (5CB) to the surface-immobilized (-COOH) groups (20). In contrast, exposure of the acidic surface to a vapor of hexylamine [ $n\text{-H}_2\text{N}(\text{CH}_2)_5\text{CH}_3$ ] (HA) before (Fig. 2, A to D) or after (see below) contact with 5CB causes a film of nematic 5CB to assume an orientation that is visually distinct. From polarized light microscopy, we determined the surface-induced orientation of the 5CB after exposure to HA to be parallel to (along) the nanometer-scale corrugation of the surface. Exposure of 5CB supported on a surface presenting methyl

**Fig. 1.** Schematic illustration of the competitive interaction of a LC and targeted low molecular weight compound for a molecular receptor hosted on a surface with nanometer-scale topography. (A) Before exposure to a targeted compound, the molecules forming the LC mesogens bind with the molecular receptor and thereby anchor the LC across the topography on the surface. (B) Binding of the targeted analyte to the surface-immobilized receptors displaces the LC from its interaction with the receptor shown in (A), and the LC orients along the topography. (C) A receptor-induced orientation of a LC that is perpendicular to a surface. (D) Binding of a targeted analyte to the surface-immobilized receptors displaces the LC from its interaction with the receptor shown in (A), and the LC orients across the topography on the surface.



Department of Chemical Engineering, University of Wisconsin, Madison, WI 53706, USA.

\*Present address: 3M Center, 3M Corporation, St. Paul, MN 55144, USA.

†To whom correspondence should be addressed. E-mail: abbott@engr.wisc.edu

REPORTS

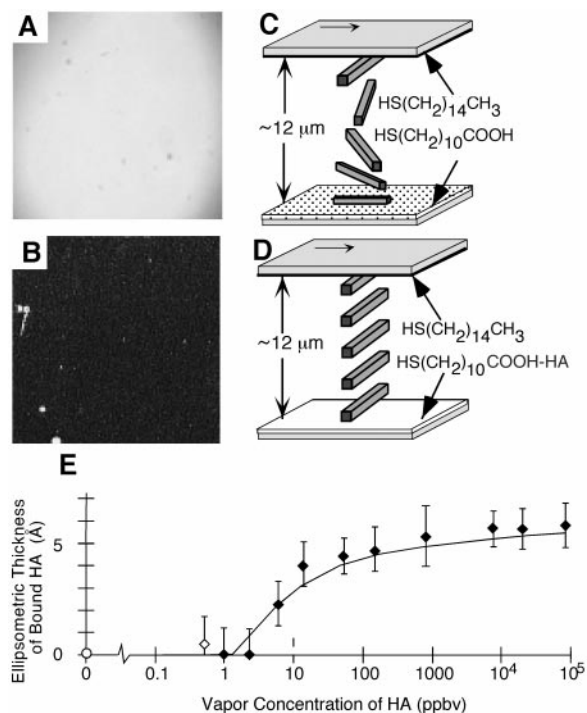
groups to HA did not lead to a change in orientation of 5CB. Similarly, exposure of 5CB supported on -COOH to water vapor, ethanol, hexanes, and dimethylphosphonate [(H<sub>3</sub>CO)<sub>2</sub>POCH<sub>3</sub>] did not trigger a measurable change in the orientation of 5CB. From this we conclude that a competitive displacement of 5CB by HA from its hydrogen bond with the carboxylic acid group leads to the change in the LC orientation (21). Since the acid-base interaction of the acid and amine has a slow off rate (14, 15), we deter-

mined the sensitivity of the LC to bound HA by measuring the amount of HA bound to the acidic surface before placement of 5CB on the surface. The change in orientation of 5CB is triggered by amounts of bound HA that possessed optical thicknesses that were below the detection limits of ellipsometry (ellipsometric thickness < 1 Å) (Fig. 2E) (22). Exposure of these surfaces to ppb concentrations of HA (for 2 min) resulted in measurable changes in orientation of the 5CB.

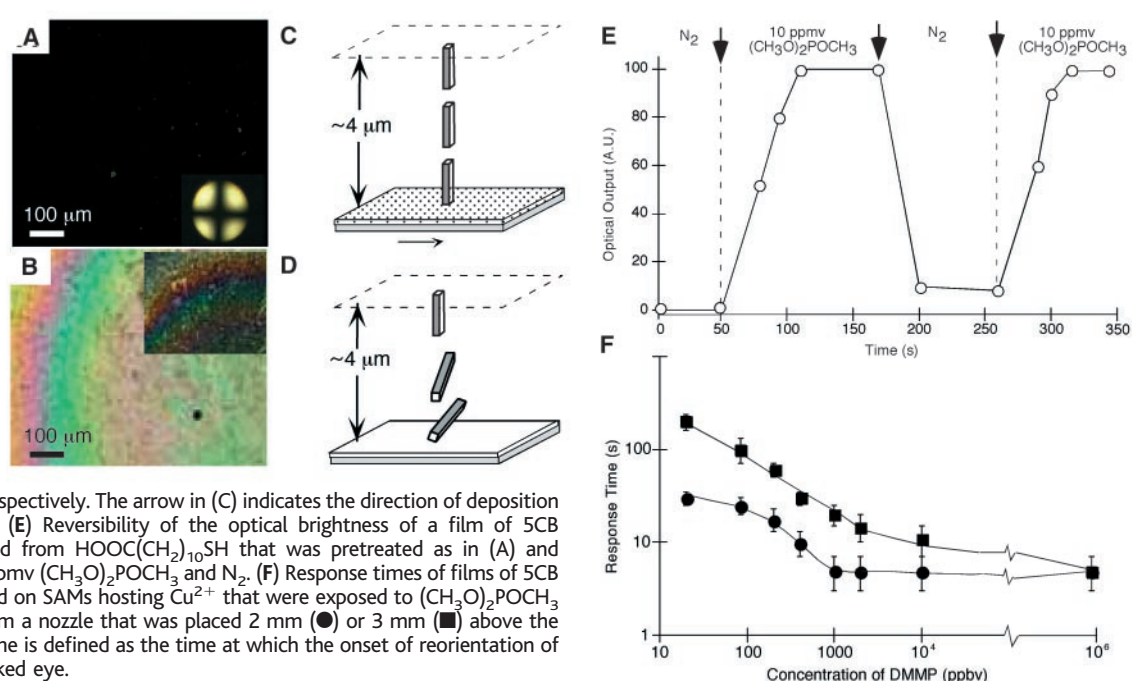
When the bound -COOH groups were pre-

treated by immersion into ethanolic solutions containing 100 mM Cu<sup>2+</sup> (23), Cu<sup>2+</sup> was incorporated into these surfaces (24), causing micrometer-thick 5CB spin-coated films to adopt an orientation that is perpendicular to the surface (Fig. 3, A and C). Mesogens not possessing a nitrile group [such as nematic phases of *n*-(*p*-methoxybenzylidene)] did not orient perpendicular to surfaces presenting Cu<sup>2+</sup>. Similarly, the incorporation of Cd<sup>2+</sup> into surfaces presenting carboxylic acid groups did not cause 5CB to assume a perpendicular orientation, consistent with the weaker binding of nitrile groups to Cd<sup>2+</sup> than to Cu<sup>2+</sup> (25). We thus conclude that complexation of the nitrile groups of 5CB with Cu<sup>2+</sup> presented at the surface gives rise to the perpendicular orientation of 5CB (26, 27). Exposure of the perpendicularly oriented film of 5CB to 300 parts per million (ppm) of water, acetone, hexanes, or ethanol did not change the optical appearance of the film of 5CB (28). However, we observed that exposure of the film to ppm to ppb concentrations of (H<sub>3</sub>CO)<sub>2</sub>POCH<sub>3</sub> resulted in an easily visualized change in the orientation of the LC (Fig. 3, B and D) (29, 30). By using polarized light microscopy and interferometry, we determined this change in orientation to be caused by a tilt (10° to 20°) of the LC away from the normal of the surface and in an azimuthal direction that is perpendicular to the nanometer-scale corrugations on the surface. We conclude that competitive binding of (H<sub>3</sub>CO)<sub>2</sub>POCH<sub>3</sub> to Cu<sup>2+</sup> hosted at the surface displaces 5CB from its weak complex with Cu<sup>2+</sup>, thereby triggering a change in orientation of the LC (31). The LC reverts to its original perpendicular orientation when

**Fig. 2.** (A and B) Optical textures (crossed polars) formed by 5CB within optical cells prepared with one surface supporting a SAM formed from H<sub>3</sub>C(CH<sub>2</sub>)<sub>14</sub>SH and an opposing surface supporting a SAM formed from HOOC(CH<sub>2</sub>)<sub>10</sub>SH: (A) before exposure of HA; (B) after exposure to 12 ppmv HA. (C and D) Schematic illustrations of the orientations of the LCs interpreted from the optical textures shown in (A) and (B), respectively. The bold arrows indicate the direction of deposition of ultrathin gold films that support the SAMs. (E) Optical thickness of HA bound to the SAM formed from HOOC(CH<sub>2</sub>)<sub>10</sub>SH as a function of the vapor-phase concentration of HA. The filled diamonds correspond to cells within which the LC did not twist (B and D), whereas the open diamond indicates a cell in which the twisted nematic phase was observed (A and C).



**Fig. 3.** Optical textures (crossed polars) formed by a film of 5CB on a surface supporting a SAM formed from HOOC(CH<sub>2</sub>)<sub>10</sub>SH that was (A) pretreated with 100 mM Cu(ClO<sub>4</sub>)<sub>2</sub> and (B) pretreated as in (A) and subsequently exposed to a vapor concentration of 900 ppmv (CH<sub>3</sub>O)<sub>2</sub>POCH<sub>3</sub> (viewed at maximum transmission). The inset in (B) shows the optical texture at maximum extinction. (C and D) Schematic illustrations of the orientations of the LCs interpreted from the optical textures shown in (A) and (B), respectively. The arrow in (C) indicates the direction of deposition of gold onto the substrate. (E) Reversibility of the optical brightness of a film of 5CB supported on a SAM formed from HOOC(CH<sub>2</sub>)<sub>10</sub>SH that was pretreated as in (A) and exposed sequentially to 10 ppmv (CH<sub>3</sub>O)<sub>2</sub>POCH<sub>3</sub> and N<sub>2</sub>. (F) Response times of films of 5CB (thickness ~4 μm) supported on SAMs hosting Cu<sup>2+</sup> that were exposed to (CH<sub>3</sub>O)<sub>2</sub>POCH<sub>3</sub> convected to the surface from a nozzle that was placed 2 mm (●) or 3 mm (■) above the film of 5CB. The response time is defined as the time at which the onset of reorientation of the LC was visible to the naked eye.



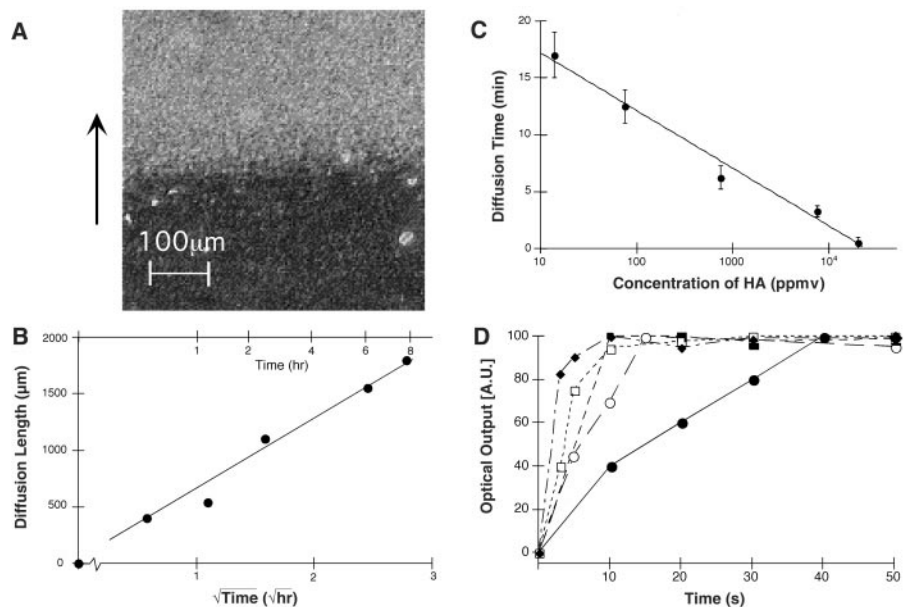


**Fig. 4.** (A) Visual appearance (using crossed polars) of a thin film of nematic 5CB sandwiched between two ultrathin gold films that possess nanometer-scale topography and support SAMs formed from either  $\text{H}_3\text{C}(\text{CH}_2)_{14}\text{SH}$  or  $\text{COOH}(\text{CH}_2)_{10}\text{SH}$ . Exposure of the bottom edge of the film of LC (as shown in the image) to a vapor of HA leads to the lateral transport (by diffusion in the direction indicated by arrow) of the HA. (B) Penetration distance (from the edge of a LC cell) of HA as a function of exposure time and as a function of the square root of exposure time. (C) Penetration time (time for the diffusion front to penetrate  $20\ \mu\text{m}$  into the cell) as a function of the vapor concentration of  $n\text{-H}_2\text{N}(\text{CH}_2)_5\text{CH}_3$ . (D) Time-dependent response (average brightness) of a film of 5CB (thickness  $\sim 4\ \mu\text{m}$ ) supported on a SAM formed from  $\text{HOOC}(\text{CH}_2)_{10}\text{SH}$  that was pretreated by immersion into an ethanolic solution of  $100\ \text{mM}\ \text{Cu}(\text{ClO}_4)_2$ . The dynamic response of the LC is shown after exposure to (●)  $20\ \text{ppbv}$ , (○)  $85\ \text{ppbv}$ , (■)  $200\ \text{ppbv}$ , (□)  $1\ \text{ppmv}$ , and (◆)  $2\ \text{ppmv}$  of  $(\text{CH}_3\text{O})_2\text{POCH}_3$  delivered from a nozzle located  $2\ \text{mm}$  from the surface of the film of 5CB.

reexposed to a  $(\text{H}_3\text{CO})_2\text{POCH}_3$ -free atmosphere (Fig. 3E). Exposure to  $\sim 20$ -ppbv concentrations (limit of dilution of our experimental setup) of  $(\text{H}_3\text{CO})_2\text{POCH}_3$  for  $\sim 20\ \text{s}$  resulted in easily visualizable changes (Fig. 3F).

Two approaches can be used to quantify either cumulative or instantaneous exposure to targeted analytes. First, measurement of the spatial extent of diffusion of HA laterally across a confined film of LC can be used to indicate cumulative exposure to time-varying concentrations of the analyte (Fig. 4, A to C). Second, we have demonstrated that it is possible to design surfaces that trigger a dynamic response of the LC that depends upon the instantaneous concentration of a targeted analyte (Fig. 4D) (32).

In summary, we have demonstrated the design of surfaces with nanometer-scale topography and receptor chemistry such that competitive interactions of mesogens and targeted analytes (organophosphonates and organoamines) to surface-immobilized receptors are amplified into chemically specific, surface-driven orientational transitions in LCs. Because a wide variety of metal ions can be patterned on surfaces within areas possessing micrometer-scale dimensions, and because LCs can be used to image surfaces on similar spatial scales, the

general approach reported here offers the possibility of rapidly screening for molecular receptors or combinations of molecular receptors for a range of targeted environmental agents. These receptors may provide the basis of measurement tools suitable for highly multiplexed determinations of personal exposure to a wide range of chemical environments.

**References and Notes**

1. B. E. Rittmann, P. McCarty, *Environmental Biotechnology: Principles and Applications* (McGraw Hill, New York, 2000).
2. M. E. Cisper, P. H. Hemberger, *Rapid Commun. Mass Spectrosc.* **11**, 1449 (1997).
3. Methods for detection of toxic compounds or their metabolites such as those based on mass-sensitive oscillators (33), microfabricated cantilevers (34, 35), fluorescence quenching (36), and enzymatic detection (37) are not suitable as the basis of personal dosimeters.
4. Past studies have reported detection of vapors (to  $\sim 1\ \text{ppmv}$ ) by their absorption into the bulk of a LC (5, 6). The bulk absorption of the analyte results in a color change caused by a change in the pitch of a cholesteric phase. The sensitivity and selectivity reported in these past studies are low.
5. E. J. Poziomek, T. J. Novak, R. A. Mackay, *Mol. Cryst. Liq. Cryst.* **27**, 175 (1974).
6. F. L. Dickert, A. Haunschild, P. Hofmann, G. Mages, *Sensors Actuators B* **6**, 25 (1992).
7. Personal dosimeters based on metallic substrates that are analyzed with a surface-enhanced Raman spectrometer have been reported (38).
8. Pieranski and co-workers have reported orientations of LCs supported on inorganic substrates (gypsum,

- mica, calcite, quartz, and silica) to change upon exposure to water, alcohols, glycols, acetic acid, and carbon tetrachloride (9, 10).
9. P. Pieranski, B. Jérôme, M. Gabay, *Mol. Cryst. Liq. Cryst.* **179**, 285 (1990).
10. B. Jérôme, Y. R. Shen, *Phys. Rev. E* **48**, 4556 (1991).
11. J. N. Israelachvili, *Intermolecular and Surface Forces* (Academic Press, New York, ed. 2, 2000).
12. R. C. Thomas, J. E. Houston, R. M. Crooks, T. Kim, T. A. Michalske, *J. Am. Chem. Soc.* **117**, 3830 (1995).
13. G. G. Guilbault, J. Das, *J. Phys. Chem.* **73**, 2243 (1969).
14. M. Wells *et al.*, *Langmuir* **12**, 1989 (1996).
15. H. C. Yang, D. L. Dermody, C. Xu, A. J. Ricco, R. M. Crooks, *Langmuir* **12**, 726 (1996).
16. V. K. Gupta, J. J. Skaife, T. B. Dubrovsky, N. L. Abbott, *Science* **279**, 2077 (1998).
17. There is a substantial need for methods that permit monitoring of biogenic amines (e.g., histamine, putrescine, and cadaverine) as markers of food degradation (most notably for fish and meat). Maximum limits of biogenic amines in foods are specified by European Economic Community regulations as  $100\ \text{mg}$  of biogenic amine per kilogram of food (39).
18. Self-assembled monolayers (SAMs) were formed on the surfaces of films of gold ( $130\ \text{\AA}$  of gold deposited onto glass microscope slides in an electron beam evaporator at an angle of incidence of  $50^\circ$  from the normal and at  $0.2\ \text{\AA/s}$ ) by immersing the films in ethanolic solutions containing  $1\ \text{mM}\ \text{HOOC}(\text{CH}_2)_{10}\text{SH}$  for 1 hour. A thin film of titanium ( $20\ \text{\AA}$ ) was used to promote adhesion between the gold and glass microscope slide.
19. J. J. Skaife, N. L. Abbott, *Chem. Mater.* **11**, 612 (1999).
20. The nitrile group of 5CB is a hydrogen bond acceptor (40).
21. We also observed that conversion of the carboxylic acid to its sodium salt leads to an orientation of 5CB that is parallel to the nanometer-scale grooves on the surface [see (40)].
22. L. S. Jung, C. T. Campbell, T. M. Chinowsky, M. N. Mar, S. S. Yee, *Langmuir* **14**, 5636 (1998).
23. The SAMs formed from  $\text{HOOC}(\text{CH}_2)_{10}\text{SH}$  were immersed for 5 min in ethanolic solutions containing  $0.1\ \mu\text{M}$  to  $100\ \text{mM}$  of  $\text{Cu}(\text{ClO}_4)_2$  or  $\text{Cd}(\text{NO}_3)_2$ . Upon removal from the ethanolic solutions, the surfaces of the slides were rinsed with ethanol and then placed under a stream of nitrogen gas to displace excess solution from the surface.
24. X-ray photoelectron spectroscopy (Perkin-Elmer PhiX 5400) was used to confirm complexation of copper and cadmium to SAMs formed from  $\text{HOOC}(\text{CH}_2)_{10}\text{SH}$  by measuring the ratio of  $\text{Cu}(2p_{3/2})$  or  $\text{Cd}(3d_{5/2})$  to the  $\text{O}(1s)$  within the SAM. We also used x-ray photoelectron spectroscopy to confirm the absence of excess salts and contaminants on the surfaces of the SAMs after their immersion in ethanolic solutions of  $\text{Cu}(\text{ClO}_4)_2$  or  $\text{Cd}(\text{NO}_3)_2$ .
25. Cadmium forms weaker coordination complexes with nitrile groups than  $\text{Cu}^{2+}$  does (41).
26. Our measurements have revealed that electrical double layers formed through the dissociation of cations from metal carboxylate surfaces can cause nematic phases of 5CB to orient perpendicular to a surface (42). This effect is only observed in films of LCs that are substantially thicker than those used in the studies reported here.
27. Infrared spectroscopic measurements have indicated that  $\text{Cu}^{2+}$  complexes with acetonitrile in the presence of ( $>1\ \text{weight}\ \%$ ) water (43, 44). We have measured the samples of 5CB used in the experiments reported here to contain  $\sim 50\ \text{mM}$  ( $\sim 1\ \text{weight}\ \%$ ) of entrained water (40).
28. R. G. Nuzzo, L. H. Dubois, D. L. Allara, *J. Am. Chem. Soc.* **112**, 558 (1990).
29. Using mass-sensitive methods, Crooks, Ricco, and co-workers demonstrated that diisopropyl methylphosphonate (DIMP) binds to  $\text{Cu}^{2+}$  hosted at the surface of SAMs presenting carboxylic acid groups (30, 33).
30. L. J. Kepley, R. M. Crooks, A. J. Ricco, *Anal. Chem.* **64**, 3191 (1993).
31. The enthalpy of binding of DIMP to  $\text{Cu}^{2+}$  has been reported to be  $-4$  to  $-5\ \text{kJ/mol}$  (13).
32. Gaseous streams of HA were prepared by gravimetric

- dilution of validated sources of 20 or 1456 ppmv HA with N<sub>2</sub> by using calibrated flow controllers. Gaseous streams of (H<sub>3</sub>CO)<sub>2</sub>POCH<sub>3</sub> were prepared by similar methods from a saturated vapor of (H<sub>3</sub>CO)<sub>2</sub>POCH<sub>3</sub> at 20°C.
33. R. M. Crooks, H. C. Yang, L. J. McEllistrem, R. C. Thomas, A. J. Ricco, *Faraday Discuss.* **107**, 285 (1997).
  34. R. Berger *et al.*, *Science*, **276**, 2021 (1997).
  35. J. Fritz *et al.*, *Science* **288**, 316 (2000).
  36. D. T. McQuade, A. E. Pullen, T. M. Swager, *Chem. Rev.* **100**, 2537 (2000).
  37. M. R. Dawood, R. Allan, K. Fowke, J. Embree, G. W. Hammond, *J. Clin. Microbiol.* **30**, 2279 (1992).
  38. T. Vo-Dinh, D. L. Stokes, *Field Anal. Chem. Technol.* **3**, 346 (1999).
  39. M. Niculescu *et al.*, *Anal. Chem.* **72**, 1591 (2000).
  40. R. R. Shah, N. L. Abbott, *J. Am. Chem. Soc.* **121**, 11300 (1999).
  41. A. E. Martell, M. Calvin, *Chemistry of Metal Chelate Compounds* (Prentice-Hall, New York, 1952).
  42. R. R. Shah, N. L. Abbott, *J. Phys. Chem B* **105**, 4936 (2001).
  43. Y. Marcus, *J. Chem. Soc. Dalton Trans.* 2265 (1991).
  44. J. F. Coetzee, W. R. Sharpe, *J. Solution Chem.* **1**, 77 (1972).
  45. Supported in part by the National Science Foundation (grants CTS-9502263 and DMR-0079983) and Office of Naval Research (Presidential Early Career Award for Scientists and Engineers to N.L.A.). N.L.A. thanks Y.-Y. Luk (University of Wisconsin) for helpful discussions.

7 May 2001; accepted 23 July 2001

## Ring Closure of Carbon Nanotubes

Masahito Sano,\* Ayumi Kamino, Junko Okamura, Seiji Shinkai

Lightly etched single-walled carbon nanotubes are chemically reacted to form rings. The rings appear to be fully closed as opposed to open coils, as ring-opening reactions did not change the structure of the observed rings. The average diameter of the rings was 540 nanometers with a narrow size distribution. The nanotubes in solution were modeled as wormlike polymer chains, yielding a persistence length of 800 nanometers. Nanotubes shorter than this length behave stiffly and stay nearly straight in solution. However, nanotubes longer than the Kuhn segment length of 1600 nanometers undergo considerable thermal fluctuation, suggesting a greater flexibility of these materials than is generally assumed.

With currently available synthetic methods (1, 2), carbon nanotubes are always grown as long strings, and this string shape is largely responsible for their immediate applications to field emission source (3), probe tips (4, 5), tweezers (6), molecular or chemical wires (7, 8), and fibrous composites (9). Despite their importance, however, there has been no effective means to shape a large number of individual carbon nanotubes in a controlled way. Chemical modification of nanotubes along logically designed pathways may be one such method. In particular, ring-forming reactions yield a result that can be easily confirmed by microscopic techniques. So far, accidental occurrences of ring structures during nanotube syntheses have been reported (10, 11). There is also a report of ring formation by physical coiling (12). We show that covalent ring-closure reactions applied to commercially available carbon nanotubes produce a sizable number of ring-shaped tubes where the tubes bond only to themselves. The rings show a narrow size distribution, which we explain by modeling the nanotubes in solution as wormlike polymer chains. The analysis gives a characteristic length scale, which classifies a given nanotube as either stiff or semiflexible in solution. Such a scale is useful for understanding aggregation behaviors, such as bundle

formations, and designing chemical modifications of nanotubes.

Commercially available pristine single-walled carbon nanotubes (SWNTs) are generally too long to be dispersed in solution and have no well-defined chemical functional groups to modify. Ultrasonically SWNTs in concentrated H<sub>2</sub>SO<sub>4</sub>/HNO<sub>3</sub> is known to cut SWNTs into many short pieces (13). Because scission occurs preferably at defect sites, this treatment produces a broad distribution of open-ended SWNTs. The cut SWNTs are then etched lightly in H<sub>2</sub>SO<sub>4</sub>/H<sub>2</sub>O<sub>2</sub> to afford oxygen-containing groups at both ends, of which some are phenolic hydroxides and carboxylic acids (14). The resulting SWNTs can be dispersed relatively well in water and dimethylformamide (DMF), although some tend to aggregate into bundles even in these dispersions. We note that dispersible amounts of SWNTs in various solvents (15, 16) depend on history of chemical treatments as well as lengths.

Ring closure can be achieved with a number of organic reactions with the oxygen-containing groups at the tube ends, provided that SWNTs have not completely collapsed or coagulated at each step of the procedure. Any processes that promote aggregation, such as filtering, should be avoided as much as possible. A possible scheme with 1,3-dicyclohexylcarbodiimide (DCC) is illustrated in Fig. 1. Raman shift of the A<sub>1g</sub> mode (17) indicates that SWNTs (laser-oven products purchased from Rice University) have a diameter of 1.2 nm. Large aggregates of

SWNTs after the acid treatments were removed by ultracentrifuge at 3500g. The remaining SWNTs in the supernatant solution were dispersed in dry DMF so that the solution was lightly colored and an excess amount of DCC was added. The mixture was stirred overnight at room temperature, after which solid materials were collected and washed on a Teflon filter. For the following statistical analysis, the reaction mixture before filtration (Fig. 2A) was used for sampling. Another reaction by modifying carboxylic acids to acid chlorides (13, 18) also produced rings but with lower yields, probably because of poorer dispersion of acid chloride SWNTs in DMF.

Atomic force microscopy (AFM) reveals rings of an average diameter of 540 nm or equivalently a contour length of 1.7 μm (Fig. 2B). A control sample of acid-treated SWNTs without reaction also produces a ring-shaped feature that is caused by physical coiling. This happens rarely, and only one or two loops, if any, are seen in the area, as shown in Fig. 2A. The diameter of coils obtained by Martel *et al.* (12) is larger on average, which may be due to the fact that the coils are open-ended whereas the present rings are closed. Once formed, rings are quite stable both chemically and physically. Ring-opening reactions, such as treating rings with dimethylaminopyridine and *n*-butylamine or NaOH, had no effect on the rings. Heating rings to 500°C under N<sub>2</sub> atmosphere for 3 hours did not open the rings. Because any oxygen-containing organic bonds should have decomposed at this temperature, it is interesting to investigate the nature of the linkage after the heat treatment.

During reproducibility experiments, we noticed that the size of rings was roughly the same even when different chemical conditions, such as water contents and different functional groups, were used. Figure 3A shows a histogram of contour lengths of rings measured directly from AFM images. There are very few rings with the contour lengths below 1.3 μm and above 2.1 μm. To explain this narrow distribution, it is necessary to understand properties of SWNTs in the reaction mixture, i.e., under what conditions two ends of a SWNT can meet by thermal fluctuation. Here, we model SWNTs in DMF by wormlike polymer chains with excluded vol-

Chemotransfiguration Project-JST, Kurume, Fukuoka 839-0861, Japan.

\*To whom correspondence should be addressed.